CCFE
CULHAM CENTRE FOR FUSION ENERGY

UK Atomic Energy Authority

UKAEA-CCFE-CP(25)30

Thomas Stokes, William Grove, JJ Weeks, James Bromley, Steven Reynolds

An Indicative Study into Vacuum Induction Melting as a Detritiation Technique for Fusion Wastes

An Indicative Study into Vacuum Induction Melting as a Detritiation Technique for Fusion Wastes

Thomas Stokes, William Grove, JJ Weeks, James Bromley,
Steven Reynolds

This paper has been submitted to
14th International Conference on Tritium Science and Technology, Ottawa, Ontario, Canada, 21 - 26 September 2025

An Indicative Study into Vacuum Induction Melting as a Detritiation Technique for Fusion Wastes

Thomas Stokes[a]*, William Grove[a], JJ Weeks[a], James Bromley[a] and Stephen Reynolds[a]

[a] *United Kingdom Atomic Energy Authority, Culham Science Centre, Abingdon, Oxon, OX14 3DB, United Kingdom*

*E-mail: tom.stokes@ukaea.uk

An Indicative Study into Vacuum Induction Melting as a Detritiation Technique for Fusion Wastes

Metal melting has been widely viewed as the most promising method for detritiating metallic waste, with its potential to release more tritium than other thermal methods. Furthermore, the homogenization of the metal post melting is expected to distribute tritium throughout the ingot, reducing hotspots in the waste form. Removing tritium from wastes is important as it makes disposing or recycling of the metal far easier. Detritiation trials conducted with stainless steel showed promising indications, with detritiation efficiencies ranging from 67% to 96%. However, the low starting activity of the charge material (<100 Bq/g) introduced high statistical variability and potential cross-contamination effects, which impacted the reliability of some data. Despite these challenges, the observed tritium removal highlights the potential of metal melting as an effective method for treating fusion-related metallic wastes. Future studies with higher activity samples and additional repetitions are planned to further investigate the impact of longer hold times and different crucible types on detritiation efficiency.

I. Introduction

Future fusion power plants will generate large volumes of metallic waste, much of it contaminated with tritium, posing significant challenges for safe disposal and recycling [1]. Waste management strategies prioritise recycling of material as per the waste hierarchy and aim to minimise overall activity of any wastes that are unable to be immediately recycled. Effective detritiation techniques are required to achieve these objectives. Thermal desorption is one such technique and has been applied widely to drive tritium from metallic wastes, with detritiation efficiencies up to 96% achieved at UKAEA's Materials Detritiation Facility[2]. While thermal desorption has proven effective, alternative approaches such as metal melting may offer additional benefits.

Metal melting offers a potential alternative, combining detritiation with simultaneous volume reduction and homogenisation of the residual activity within the ingot [3]. This helps to improve packing efficiency and reduce the characterisation burden of the resultant waste form.

This study investigates Vacuum Induction Melting (VIM) as a detritiation method for low-activity stainless steel. VIM furnaces use alternating current (AC) supplied through an induction coil surrounding the metal workpiece. The AC coil creates an alternating magnetic field, which in turn induces eddy currents in the workpiece, producing heat via ohmic heating. The control of melt environment is of interest for detritiation and waste management, since surface oxide formation can inhibit tritium release from bulk when heating metals in the presence of oxygen [4] [5]. The addition of small quantities of hydrogen gas to the melt chamber may also promote detritiation via isotopic exchange reactions [3].

Initial studies with VIM furnaces have indicated that metal melting under a hydrogen atmosphere can achieve detritiation factors in stainless steel greater than previously used techniques and is thus capable of reclassifying waste samples from ILW to LLW classification due to a reduced tritium inventory [3]. In addition, with the high degree of control on the atmosphere (composition) and heating offered with a VIM furnace, it is expected that secondary waste generation from slag and dust can be significantly reduced compared to other metal melting techniques.

Treatment of metals in a VIM furnace may thus prove to be a useful alternative or addition to existing detritiation processes, following further study of the process. This study aims to evaluate the potential of VIM for detritiation of low-activity stainless steel, providing initial insights into its effectiveness and operational considerations.

II. Method

The key aim of this work was to investigate the detritiation effectiveness of VIM. In addition, the effect on detritiation of varying three melting parameters was explored as part of this trial. This included altering the gas used, the crucible type, and the melt heating profile in single replicate trials.

The furnace used is shown in Figure 1, with specifications given in Table 1.

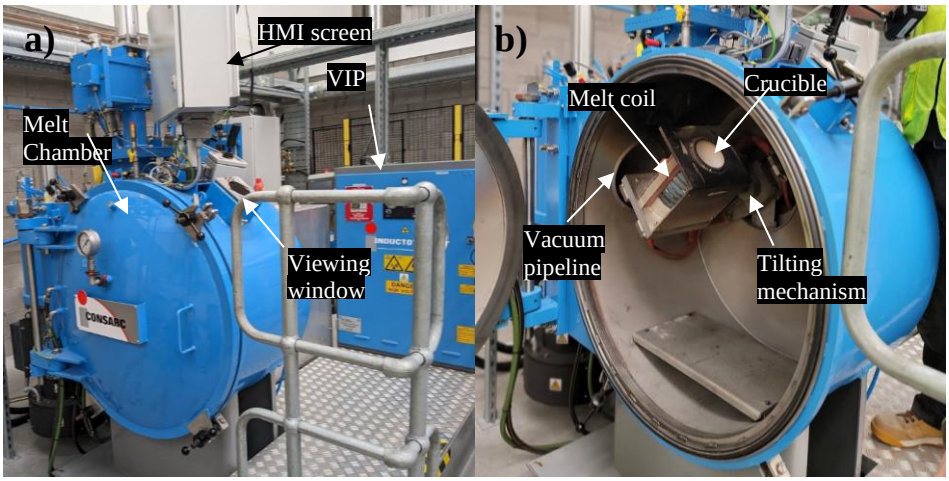

Figure 1. Image of the melting furnace showing a) the melt chamber and VIP supply cabinet, and b) an inside view of the melt chamber.

Table 1. Specifications of the VIM furnace used in these trials.

Component	Details
Furnace Type	4kg capacity VIM furnace (Consarc Engineering Ltd)
Power Supply	Inductotherm VIP unit, up to 20kW, max 10kHz
Vacuum System	Rotary + roots blower: ~10^{-3} mBar Oil diffusion pump: ~10^{-5} mBar
Backfill Capability	Up to 100 mBar via cylinder gas supply
Gases Used	Nitrogen, Argon, 2.5% Hydrogen in Argon (supplied by BOC)
Crucibles	Sourced from Capital Refractories, AL68S 5050 liner, AL97 1017 crucible, and ZC93 1017 crucible [6].
Temperature Monitoring	Fluke Endurance E1RL Infrared Pyrometer CCPI Europe K type insulated dip thermocouple (TC)

Temperature was monitored using a Fluke Endurance E1RL infrared pyrometer, and final melt temperature measured with a K-type insulated thermocouple (CCPI Europe) mounted on a pneumatic extension arm for immersion. The detritiation trials used tritiated stainless steel previously processed through UKAEA's Materials Detritiation Facility, with initial activity <100 Bq/g. This designation placed the material Out of Scope under Environmental Permitting Regulations [7], allowing work without a permit, though a Local Enforcement

Position from the Environment Agency was required due to the absence of UK limits for gaseous tritium emissions during melting [7]. Pre-melting samples from separate bulk metal pieces were cut using a Marvel Series 8 Mark 2 vertical band saw with Q8 Brunel XF 343 soluble coolant to minimise tritium release and analysed for tritium. Mean activity for the charge material was then calculated (Table 2). The remaining bulk steel was cut (~4 × 4 × 1 cm) using the same method to create the charge material for the melting trials. Post-melt ingots were also sampled using the same method.

Table 2. Activity and masses of tritiated steel samples before melting.

Piece ID	Piece Mass (g)	Sample Activity Concentration (Bq/g)	Sample Mass (g)	Mean Piece Activity Concentration (Bq/g)
1A	8120	20.2 ± 2.3	10.729	30.3 ± 1.9
		19.7 ± 2.2	10.74	
		51.2 ± 4.5	11.018	
1B	8041	47.2 ± 4.4	9.852	37.2 ± 2.1
		33.0 ± 3.2	10.791	
		31.3 ± 3.1	10.383	
3C	7357	15.8 ± 2.0	10.992	30.7 ± 1.9
		36.5 ± 3.6	10.969	
		39.7 ± 3.8	10.556	

The analysis of samples pre and post melting was undertaken at UKAEA Tritium Analysis Laboratory (TAL), utilising Raddec Gen IV Pyrolyser with 2 water bubblers in series to capture tritium. A blank sample run was performed before each analytical run to show any residual or background tritium expected in the system. Samples were loaded into separate working tubes in the pyrolyser, which was then heated to 800°C and held for 4 hours, before cooling. Bubbler water containing the captured tritium was analysed via Liquid Scintillation Counting (LSC).

Melting process parameters and outputs are summarised in Table 3. Some final temperature readings from the immersion thermocouple were erroneous, likely due to probe fouling or insufficient immersion depth in small melt volumes. Data for Melt 8 were lost due to a

technical error.

Metal was weighed out into the selected crucible, placed inside the backup crucible in the melt chamber and the chamber evacuated to ~2E-2 mBar. Power was then delivered to the melt coil according to Table 4.

Table 3. Key parameters and outputs from the tritiated steel melts. Values in italics represent erroneous values.

Test Condition	Melt No.	Crucible	Gas	Mass (kg)	Mean Piece Activity Concentration (Bq/g)	Melt Profile	VIP kW.h	Pyrometer Max (°C)	DipTC Max (°C)	Melt Time (hh:mm:ss)
Gas	1	AL L	Ar	2.648	37.2 ± 2.1	Standard	6.05	1462	1434	00:56:59
	2		N	2.186			5.77	1482	*1340*	00:55:41
	3		H_2/Ar	2.242			6.18	1563	1403	00:58:06
Crucible	4	AL L	Ar	2.432	30.7 ± 1.9	Standard	5.43	1473	1434	00:55:01
	5	AL C		1.996			5.13	1463	*684*	00:54:31
	6	ZC C		2.006			4.67	1542	1490	00:51:51
Temp. Holds	7	AL L	Ar	2.352	30.3 ± 1.9	10 min hold at 700°C	7.76	1467	*1324*	01:13:54
	8			2.336		10 min hold at 1450°C	n/a	n/a	n/a	~01:04:00
	9			2.396		20 min hold at 1450°C	5.48	1475	*1288*	01:03:28

Table 4. Power curve applied for tritiated steel melts

Power	3kW	5kW	7kW	10kW	12kW
Duration	12 min	20 min	10 min	7 min	Until molten

During the 3 kW heating phase, the vacuum pipeline remained open for 10 min before being closed and the chamber backfilled to 100 mbar with the gas specified in Table 3. After melting, induction power was switched off and the metal cooled in the chamber. The chamber was then cycled three times with fresh air and vacuum to remove residual tritium prior to ingot removal. Nine ingots were sub-sampled and analysed via pyrolysis followed by liquid scintillation counting, as previously described. Figure 2 illustrates the intended sampling layout for ingots; however, the actual melt profiles (Figure 4) varied slightly in surface area due to differences in charge amounts and crucible dimensions. As samples needed to meet a minimum size requirement, this resulted in different numbers of rows between melts

(typically four rows instead of five). The sampling approach remained consistent in targeting multiple positions across the ingot surface. The top row (denoted [X,1] in Figure 2.C) represents the ingot surface that remained uncovered by the crucible and was directly exposed to the atmosphere during the melting process. Central sampling was not possible due to void formation during melting.

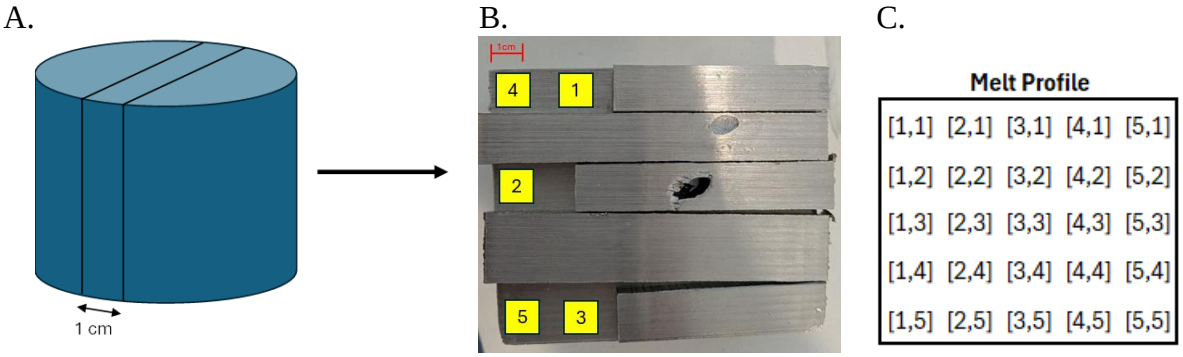

Figure 2. A. Schematic sampling plan (five rows shown for illustration; actual melt profiles varied, see Figure 3) with example void space displayed. B. An image of Melt 9, showing sample locations on a melted ingot. C. A schematic showing sample position coordinates.

Detritiation factors and efficiencies were calculated using equations (1) and (2), where DF = Detritiation Factor, E = Detritiation Efficiency; C_0 = mean tritium inventories in pre-melt samples; and CF = mean tritium inventories in post-melt samples. The distribution of the residual tritium inventory was also assessed by comparing the activity within the 5 samples taken from each ingot.

$$DF = \frac{C_0}{C_F} \quad (1)$$

$$E = 1 - \frac{C_F}{C_0} \quad (2)$$

Voids in melt cross-sections (Figure 2) were analysed using ImageJ. Automated thresholding was unsuitable due to reflective, textured surfaces, so manual region-of-interest selection was applied to ensure accurate delineation, following best practice for metallic defect analysis. Only surface area was measured, providing an indication of void size under different

conditions.

Following Melts 1 and 9, surface contamination smears were collected and analysed by liquid scintillation to assess tritium transfer to equipment and surroundings. Areas sampled included: ingot exterior (~275 cm^2), crucible interior (~534 cm^2), melt coil top (~459 cm^2), vacuum pipeline filter (~284 cm^2), chamber wall (~900 cm^2), and floor below chamber door (~900 cm^2).

III. Results

The results of the tritium analysis and respective detritiation factors and efficiencies are shown in Table 5.

The results for Melt 1 and Melt 2 were higher than the starting activity concentration of the material. Although the pyrolyser working tubes were subject to a clean-up run prior to the samples being analysed, the activities reported were still an order of magnitude higher than the activity of the pre-samples. This is expected to be due to cross contamination between analytical runs. Therefore, the results for these melts have been deemed void and removed from this analysis. This means that no direct comparison is possible for detritiating the same material under different gas conditions.

Table 5. Tritium analysis results from all tritiated steel melts. *Uncertainty confidence factor (k) = 2.

Melt	Crucible	Gas	Melt Profile	Melt Mass (g)	Mean Piece Activity Concentration (Bq/g)	Pyrolyser	Coordinate in Melt Ingot	Sample Mass (g)	Sample Activity (Bq/g)	Uncertainty (Bq/g)*	Mean Sample Activity (Bq/g)	Detritiation Factor	Detritiation Efficiency (%)
3	AL Liner	H_2/ Ar	Standard	2242	37.2 ± 2.1	3	[4,1]	7.939	1.5	0.7	2.4 ± 0.4	15.7	94 ± 1
							[5,2]	7.806	1.8	0.7			
							[4,4]	7.795	2.1	0.8			
							[5,1]	7.978	4.7	1.1			
							[5,4]	8.092	1.8	0.7			
4	AL Liner	Ar	Standard	2432	30.7 ± 1.9	3	[4,1]	8.539	0.8	0.5	1.1 ± 0.3	27.5	96 ± 1
							[5,2]	8.692	0.9	0.5			
							[4,4]	8.572	1.1	0.6			
							[5,1]	8.306	2.0	0.7			
							[5,4]	8.416	0.9	0.5			
5	AL Crucible	Ar	Standard	1996	30.7 ± 1.9	1	[4,1]	8.714	0.4	0.5	9.6 ± 0.8	3.2	69 ± 3
							[5,2]	8.317	25.2	2.9			
							[4,4]	7.492	19.2	2.5			
							[5,1]	8.695	2.5	0.8			
							[5,4]	7.555	0.5	0.6			
6	ZC Crucible	Ar	Standard	2007	30.7 ± 1.9	2	[2,1]	8.083	6.6	1.3	10.0 ± 0.8	3.1	68 ± 3
							[5,2]	7.967	15.7	2.2			
							[4,4]	7.217	6.6	1.4			
							[1,1]	7.708	13.0	1.9			
							[5,4]	7.195	8.0	1.6			

							[4,1]	8.432	0.7	0.6			
							[5,2]	8.457	0.6	0.6			
7	AL Liner	Ar	20 min hold at 1450°C	2359	30.3 ± 1.9	3	[4,4]	8.509	0.8	0.6	0.8 ± 0.3	36.1	97 ± 1
							[5,1]	8.558	1.5	0.7			
							[5,4]	8.262	0.6	0.6			
							[4,1]	8.964	0.4	0.5			
							[5,2]	8.011	5.4	1.2			
8	AL Liner	Ar	10 min hold at 1450°C	2359	30.3 ± 1.9	1	[4,5]	8.521	6.4	1.3	2.8 ± 0.4	10.8	91 ± 1
							[5,1]	9.138	1.4	0.6			
							[5,5]	8.353	0.5	0.6			
							[4,1]	8.48	3.2	0.9			
							[5,3]	8.074	12.2	1.9			
9	AL Liner	Ar	10 min hold at 700°C	2359	30.3 ± 1.9	2	[4,5]	8.57	1.0	0.6	4.3 ± 0.5	7.0	86 ± 2
							[5,1]	8.351	0.9	0.6			
							[5,5]	8.271	4.2	1.0			

The distribution of any residual tritium in the ingots was of interest to assess the homogeneity of activity in the ingot. This is plotted in Figure 3 as a cross section of each ingot.

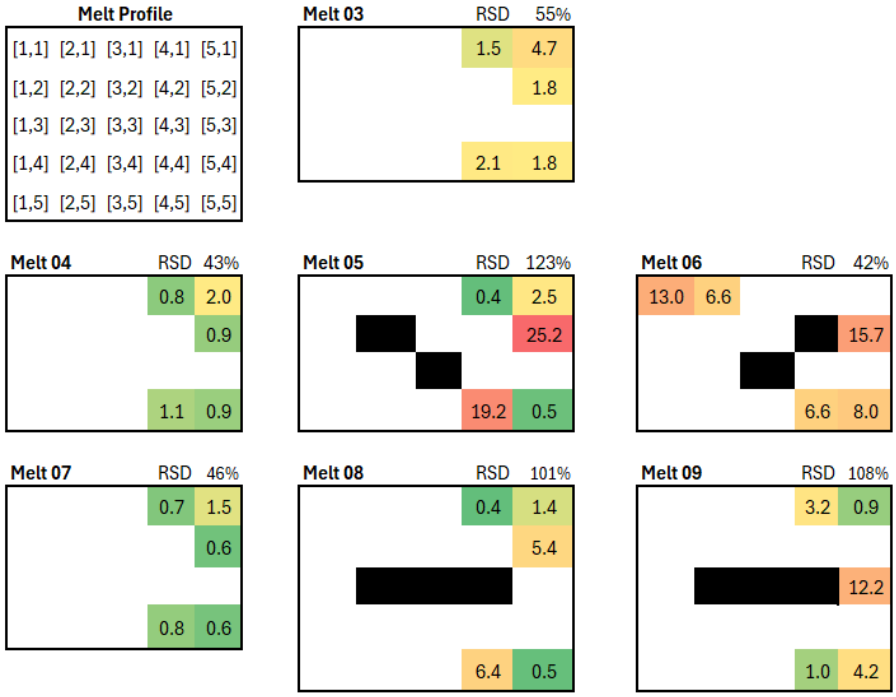

Figure 3. Plots illustrating the residual tritium distribution (Bq/g) in the detritiated steel ingots. Black bars relate to recorded void space positions. Void spaces existed but were not recorded for Melts 3, 4, and 7. RSD = Relative Standard Deviation.

The results for the void space analysis results are shown in Table 6.

Table 6. Void space surface area measurements for recorded ingots.

Melt	**Condition**	**Ingot Surface Area (cm^2)**	**Void Surface Area (cm^2)**	**Void space (%)**
5	AL Crucible	112.204	6.408	6
6	ZC Crucible	143.843	8.614	6
8	10 min hold at 1450°C	173.509	12.75	7
9	10 min hold at 700°C	181.916	2.744	2

The results for the contamination smears are shown in Table 7. All smear results were below the analytical limit of detection (LoD); therefore, reported concentrations represent LoD values rather than measured contamination.

Table 7. Tritium contamination smear locations and results for Melt 1 and Melt 9. The results

Smear Location	Smear area (cm^2)	Concentration (Bq/cm^2)	
		Melt 1	Melt 9
Ingot	275 cm^2	<0.95	<0.95
Crucible	534 cm^2	<0.49	<0.49
Melt Coil	459 cm^2	<0.57	<0.57
Filter	284 cm^2	<0.92	<0.92
Chamber Wall	900 cm^2	<0.29	<0.29
Floor	900 cm^2	<0.29	<0.29

IV. Discussion

The results indicate metal melting to be an effective method for the detritiation of stainless steel, with detritiation efficiencies ranging from 68 to 97%. This is notable given the material had already undergone thermal treatment, which would have removed surface-bound tritium. These results indicate that metal melting can extract tritium from the bulk material, a capability not achievable with existing thermal techniques.

The LSC LOD is 100 Bq/L (≈0.4 Bq/g for our sample size). Sample activities are <100 Bq/g above the LOD, resulting in high relative statistical uncertainty. As activity approaches the LOD, the signal-to-noise ratio decreases, making it harder to distinguish true activity from background. Consequently, small changes in measured activity can produce large percentage variations

Due to the low activity of the charge material, achieving very high detritiation

efficiencies (>99%) was not possible because of the pyrolyser detection limits. Potential low-level cross-contamination also had a significant impact on results. Pyrolyser 3 recorded the lowest post-melt tritium concentrations, yielding efficiencies >90%, whereas Pyrolysers 1 and 2 were lower. This may reflect residual tritium from previous samples in their work tubes despite clean-up runs. Actual post-melt tritium levels in these samples could therefore be lower than measured, implying higher true efficiencies.

Averaging residual tritium for Melts 3–9 shows similar values across vertical positions: top (33 ± 15%), centre (32 ± 14%), and bottom (35 ± 6%). Uncertainties are expressed as the standard error of the mean (SEM) multiplied by a coverage factor (k) of 2. This indicates no significant vertical stratification. Horizontally, edge samples (66 ± 50%) appear higher than centre samples (34 ± 25%), but large variance at the edges prevents statistical significance at the 95% confidence level. Overall, melting achieves effective vertical mixing, while horizontal analysis suggests localized edge heterogeneity, with higher mean tritium and greater uncertainty compared to the bulk centre.

One hypothesis for this effect is that as the surrounding metal begins to solidify, tritium remaining in the molten phase may migrate radially outward, driven by thermal and concentration gradients. Given that the edges cool and solidify earlier than the centre, they may serve as preferential trapping sites for tritium, offering an explanation for the elevated concentrations observed compared to the centre. The shrinkage voids or gas bubble cavities observed at the centre of the ingots indicate regions that solidified last. These pore spaces should be investigated more in future studies as could contain elevated levels of tritium in the gas phase.

Outliers were observed in Melts 5 (mid-centre and bottom-centre) and Melt 6 (mid-

centre), possibly due to cross-contamination. These values were identified using a box and whisker plot (Figure 4).

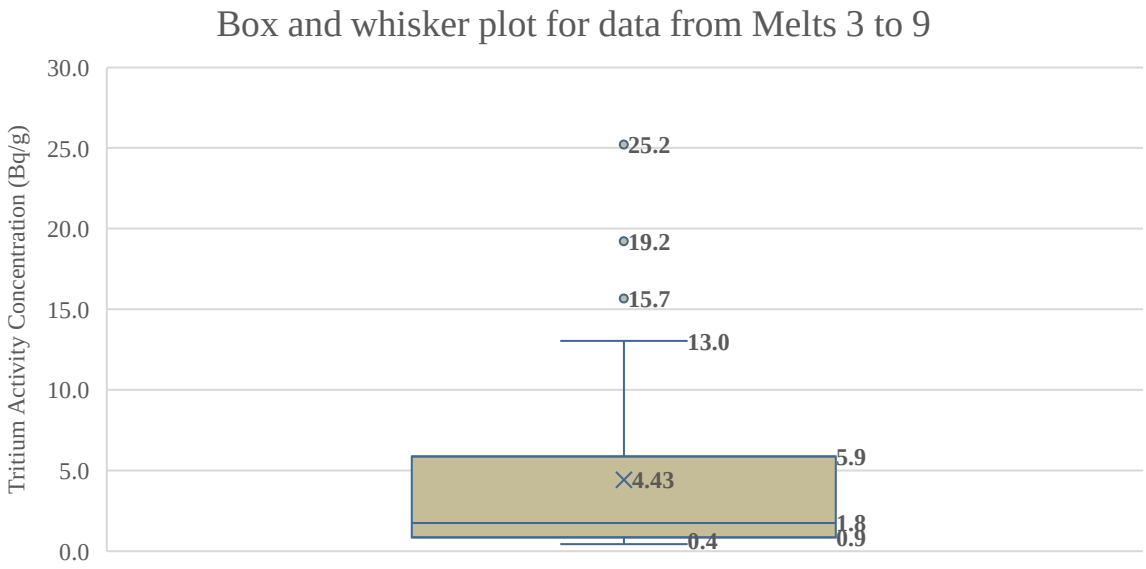

Figure 4. Box and whisker plot for the data from melts 3 to 9, showing the outlying values of 16, 20 and 26 Bq/g. Here, the minimum = 1, first quartile (Q1) = 1, median = 2, third quartile (Q3) = 6.5. Outliers are typically shown as points which are above the upper fence (13), which is calculated as Q3 + 1.5 x interquartile range (IQR).

Due to these outlier values being lower than the starting charge material specific activities, they have been included in this analysis as the values show tritium removal from the metal. Further trials are required to investigate this more.

Melts 7–9 tested the effect of dwell time on detritiation efficiency and homogeneity. Melt 7 (20 min at 1450 °C) achieved the highest efficiency (97%) and lowest variability (46% RSD), outperforming Melt 8 (10 min at 1450 °C) and Melt 9 (10 min at 750 °C). Melt 4 (no dwell time) showed similar performance to Melt 7 (96% efficiency, 43% RSD), indicating that reaching 1450 °C is the primary factor driving detritiation, while dwell time has minimal influence under these conditions. The results from these melts are summarised in Table 8.

Table 8. Detritiation results comparing different hold times and temperature.

Hold Time analysis	Melt 4 - no hold time	Melt 7 - 20 min hold at 1450°C	Melt 8 - 10 min hold at 1450°C	Melt 9 - 10 min hold at 750°C
Detritiation Factor	27.5	36.1	10.8	7
Detritiation Efficiency	96%	97%	91%	86%
Relative Standard Deviation	43%	46%	101%	108%

Ingot surface areas varied due to differences in charge mass and crucible geometry. Melt 9 exhibited a void area 4–5% smaller than other melts (Table 6). This melt included a 10 min hold at 700 °C before heating to maximum temperature, likely reducing void size through hydrogen degassing. Holding the ingot at 700ºC allowed for degassing/drying of the charge metal and ceramic crucible in solid state [8] [9]. This removed moisture on the large surface area of the charge material with enough time to desorb and diffuse away before the liquid melt forms. As the melt cools upon reaching 1400ºC, there is minimal chance for the ingot to re-absorb any hydrogen released from the metal and the crucible, resulting in a void caused purely by thermal contraction.

When heated directly to 1400 °C, released hydrogen becomes trapped in the melt as the surface-to-volume ratio is lower [10] and solubility in liquid stainless steel is higher (0.032 wppm/K) than solid steel (0.0034 wppm/K) [3]. Upon cooling, the solubility of the hydrogen within the metal drops, causing bubbles to form, which migrate to the thermal centre and merge with the shrinkage voidage, increasing its size. In commercial VIM processes, the surface area in the molten state is maximised by techniques such as ladle degassing and steam degassing.

The tritium smears came back as LOD, showing no tritium contamination had spread through the melting process. This was expected due to the low total activity input into the furnace, as well as the measurements from the dust experiments showing very little contamination in the furnace following a melt. Repeating this exercise with higher

tritium activities will prove useful to see if the tritium is retained in the equipment after the melting process has ended.

V. Conclusion

A total of 9 melts were performed using stainless steel with low levels of tritium (<100 Bq/g) to test the furnace as a detritiation method. Due to the starting activity of the charge material being low, the results were subject to high relative statistical variability and the effect of low levels of cross contamination. Results for Melt 1 and 2 were discarded due to cross contamination.

Melts 3 – 9 all showed tritium removal following the melting process, with detritiation efficiencies ranging from 68 to 97%. With such low starting activity and knowing that the charge material had already been subject to a thermal treatment, to be able to achieve high detritiation efficiencies is significant for fusion waste management and these results indicate that metal melting could be a useful mechanism for treating metal wastes.

Analysis confirms the ingots are homogeneous from top to bottom. Horizontal analysis suggests a potential accumulation of tritium at the edges; however, high variance in the edge material makes this difference statistically indistinguishable from the centre.

For all the parameters tested, clear trends were not observed other than it is possible to remove high percentages of tritium via induction melting. With higher activity samples and more repeats the trend of longer hold times and different crucible types could be studied in more detail.

Further studies into metal melting should focus on trials using charge material with higher tritium activities to remove the influence of cross contamination, LOD, and

relative statistical variability. Repeating the experiments conducted in this paper with higher activity charge material would allow for clearer conclusions on the impact of parameters like crucible type and hold time on detritiation and void space to be made.

V. Acknowledgements

This work has been carried out at UKAEA in collaboration with the Tritium Analysis Laboratory (TAL) and Materials Detritiation Facility (MDF).

This work was partly funded by and undertaken in collaboration with the ITER project.

This work has been (part-) funded by the EPSRC Fusion Grant 2022/27 [grant number EP/W006839/1]. To obtain further information on the data and models underlying this paper please contact PublicationsManager@ukaea.uk*.

VI. References

[1] L. Di Pace, L. El-Guebaly, B. Kolbasov, V. Massaut, and M. Zucchetti, "Radioactive Waste Management of Fusion Power Plants," *CORE.ac.uk*, pp. 303–328, 2012, [Online].

[2] M. Kresina *et al.*, "Preparation for commissioning of materials detritiation facility at Culham Science Centre," *Fusion Engineering and Design*, vol. 136, pp. 1391–1395, Nov. 2018, doi: 10.1016/j.fusengdes.2018.05.019.

[3] A. N. Perevezentsev *et al.*, "EXPERIMENTAL TRIALS OF METHODS FOR METAL DETRITIATION FOR JET," *Fusion Science and Technology*, vol. 52, pp. 94–99, 2007.

[4] Pacenti P, Edwards R A H, and Campi F, "Detritiation of Graphite and Beryllium plasma facing components," *Fusion Technology*, pp. 1705–1708, 1996.

[5] T. Stokes, M. Damjanovic, J. Berriman, and S. Reynolds, "Detritiation of JET Beryllium and Tungsten," *Fusion Science and Technology*, pp. 1–7, Jun. 2023, doi: 10.1080/15361055.2023.2219826.

[6] Capital Refractories, “Crucibles and Related Products,” Apr. 2013.

[7] Environment Agency, *The Environmental Permitting (England and Wales) Regulations 2016*. United Kingdom, 2016.

[8] I. Vicario, “Induction Melting Process Optimization,” 2020.

[9] J. F. O’Hanlon, “Materials in Vacuum,” in *A User’s Guide to Vacuum Technology*, Wiley, 2003, pp. 289–312. doi: 10.1002/0471467162.ch16.

[10] VAC AERO, “Vacuum Degassing of Steel,” https://vacaero.com/information-resources/vac-aero-training/101401-vacuum-degassing-steel.html.